Nature of Hydrogen Interaction and Saturation on Small Titanium Clusters

P. Tarakeshwar,* T. J. Dhilip Kumar, and N. Balakrishnan

Department of Chemistry, University of Nevada Las Vegas, 4505 Maryland Parkway, Las Vegas, Nevada 89154

Received: August 21, 2007; In Final Form: December 18, 2007

This work explores the nature of interaction and saturation of hydrogen molecules on small titanium clusters using ab initio calculations. Molecular dynamics simulations and ensuing charge density maps were used to gain insight into the key steps involved in dissociation of the hydrogen molecule on the metal clusters. The mechanistic insights gleaned from these simulations were subsequently utilized to obtain realistic models of the hydrogen saturated titanium clusters. It was found that the most stable hydrogen saturated titanium clusters involve hydrogen multicenter bonds. The observed peaks in the experimental mass and photoelectron spectra of hydrogen saturated titanium clusters are attributed to structures possessing hydrogen multicenter bonds. Hydrogen multicenter bonds are also ascribed to the origin of the broad shoulder in the vibrational spectra of hydrogen cycled Ti-doped $NaAlH_4$ reported in a recent study.

1. Introduction

There is considerable interest in the design and development of complex metal hydrides as hydrogen storage media.[1−6] One of the most promising systems in this regard is the titanium-doped sodium Alanate system.[2,3,7,8] Several studies have delved into the role of each of the constituent atoms in the hydrogen adsorption and currently there is a broad consensus that the titanium atom plays a key role in the hydrogen adsorption.[9−25] Indeed, recent experimental studies indicate that the titanium atom does not enter substitutional or interstitial sites in the $NaAlH_4$ lattice.[12,22,23,26] Although several studies suggest that the enhanced activity of these systems stems from the titanium atoms or associated titanium clusters located on/near the surface,[12,22,23,25] there is relatively little information on how hydrogen adsorption modulates the properties of both isolated titanium clusters and titanium-doped sodium Alanate.

On the other hand, it is fairly well-known from several experimental and theoretical investigations that complexes involving transition metal clusters and hydrogen display a kaleidoscopic array of size-selective interactions, which are dependent not only on the chemical nature of the metal atoms involved but also on the constituent charge and hydrogen coverage.[27] Efforts to identify the size dependence of hydrogen adsorption on small titanium clusters have led to a recent work from this group on the dissociative chemisorption of H_2 on small Ti_n ($n = 2-15$) clusters.[28] In the course of that work, it was realized that some of the isolated clusters (like Ti_4, Ti_7, and Ti_{13}) exhibit an enhanced energetic stability. In terms of adsorption of a single hydrogen molecule, the largest chemisorption energy was exhibited by the highly symmetric Ti_4 (T_d) and Ti_{13} (I_h) clusters. It would therefore be interesting to investigate on whether these trends in chemisorption energy persist as the number of adsorbed hydrogen molecules is increased. However, one of the major problems in this context is the location of the hydrogen atoms on the titanium clusters.

Most earlier investigations of hydrogen adsorption on titanium containing systems have predominantly focused their attention on the energetics of adsorption on pristine bulk surfaces,[29−32] with the positions of the hydrogens being determined by the number of electrons they can ideally share with the surface titanium atoms. Thus, Cremaschi and Whitten studied the chemisorption of H_2 on Ti (0001) surface using ab initio configuration interaction theory and concluded that the dissociation of H_2 occurs at a distance significantly above the surface and the bonding between the two is mainly due to the sharing of the 4s electrons of titanium with the hydrogen atom.[32] These studies indicate that the energy for the binding of a single hydrogen atom to the titanium surface is 3.0 eV. A latter study of the adsorption of hydrogen on a clean titanium surface yielded values in the range of 3.0−4.7 eV.[33]

Energetic considerations, however, preclude the dissociative chemisorption of hydrogen on a single titanium atom because the binding energy of TiH (1.96 eV) is much smaller than that of H_2 (4.48 eV). The presence of an additional titanium atom, as in the case of the titanium dimer, however, energetically facilitates the dissociative chemisorption of hydrogen.[28] The Pauli repulsion between the filled molecular and substrate orbitals would require an activation energy for dissociative adsorption of hydrogen on titanium.[34] Harris and Andersson have argued that the empty d states of the transition metal enables the formation of M−H bond without the strong involvement of the repulsive s-type metal orbitals.[35] Latter work, however, indicates that the above theory is only valid at long distances and activation energies do appear for interactions dominated by covalent effects.[36,37]

To date, most theoretical studies involving hydrogen saturation on transition metal clusters have been based on systems wherein the hydrogens are randomly attached to the cluster. Although these studies are useful in obtaining estimates of hydrogen adsorption capacities, in most cases the results cannot be reconciled to the experimental observations. Another facet of small titanium clusters which has attracted little attention but has a bearing on the structures of the hydrogen saturated clusters is the difficulty in assigning the electronic state of the lowest energy cluster.[38]

Against this background, we explore the nature of hydrogen saturation in small titanium clusters employing ab initio methods. We initially carried out an ab initio molecular

* E-mail: tarakesh@unlv.nevada.edu.

10.1021/jp076718j CCC: $40.75
Published on Web 03/01/2008

dynamics simulation of the interaction of hydrogen with small titanium clusters. On the basis of the detailed analysis of the charge density profiles of the structures obtained in the course of the dynamics simulation, we have been able to identify the sites at which hydrogen could be preferentially adsorbed on these small titanium clusters. This information is subsequently used to generate structures of several plausible hydrogen saturated titanium clusters and determine the corresponding chemisorption energies and vibrational frequencies. Given the current interest in titanium decorated systems owing to their potential utility as high-density hydrogen storage media, we believe that the current study would provide a detailed understanding of the various steps involved in the dissociative chemisorption of hydrogen on transition metal clusters. In the next section, we provide the details of the computational methodology. This is followed by a discussion of the results and a summary of our findings.

2. Computational Details

All the calculations reported in this study have been carried out using the Becke-3 Lee Yang Parr (B3LYP) hybrid functional.[39] Complete geometry optimizations were carried out using the 6-31G*, aug-cc-pVDZ, and the Stuttgart relativistic small core effective core potential (SRECP) basis sets for the titanium atoms.[40−42] In calculations involving the latter basis set, effective core potentials (ECPs) were included and the 6-31++G** basis set was used to represent the hydrogen atom. The vibrational frequencies were evaluated using the 6-31G*, 6-31G**, and aug-cc-pVDZ basis sets for the smaller Ti_4 clusters. However, the 6-31G* basis set was only used for evaluating the vibrational frequencies of the larger Ti_7 and Ti_{13} clusters. We also carried out single point calculations at the second-order Møller−Plesset (MP2) level of theory on some of the smaller systems. For the sake of brevity, we denote only the metal basis set when describing the calculations. Because earlier calculations on isolated metal clusters indicated that the singlet state was more stable in the case of Ti_7 and Ti_{13},[28] all calculations on these systems were carried out on this state. In the case of Ti_4, we carried out calculations on both the triplet and singlet states. Although the triplet is the ground state in the isolated metal cluster, hydrogen saturation stabilizes the singlet state. Thus, in the case of the hydrogen saturated Ti_4 clusters, all the calculations were carried out on the singlet state.

The ab initio molecular dynamics simulation was carried out using the atom-centered density matrix propagation (ADMP) molecular dynamics method.[43] This method is particularly suited because it enables the use of any density functional, including hybrid functionals. Thus, one can readily reconcile the results with those obtained from conventional electronic structure calculations. Additionally, it enables the explicit treatment of all the electrons in the system. The B3LYP hybrid density functional was used to evaluate the energies in the ADMP simulations. All the dynamic simulations were carried out using the Stuttgart relativistic small core ECP basis for the titanium and the 6-31++G* basis for the hydrogen atom.[42] The ADMP trajectories were integrated with a step size of 0.1 fs and a $\mu_{valence}$ of 0.1 amu bohr ^{2} for the fictitious mass of the electronic degrees of freedom. The simulations were carried out for about 150 fs for simulations involving the Ti_4 cluster.

All the charges reported in this study were evaluated using the Natural Bond Orbital Method.[44] The topological analysis of the electron densities of various intermediate structures was carried out using the atoms-in-molecules (AIM) method of Bader.[45]

3. Results and Discussion

In the earlier study on pure titanium clusters, purely energetic considerations were used to infer the enhanced stability of the Ti_4, Ti_7, and Ti_{13} clusters.[28] Incidentally, these clusters have significantly higher HOMO−LUMO gaps as compared to the neighboring clusters.[28] It is well-known that large HOMO−LUMO gaps together with low electron affinities and high ionization potentials are responsible for the enhanced stability of magic-number metal and metal-hydrogen clusters.[46,47] An interesting but an overlooked facet of these clusters is the coordination number of titanium. Thus, in their energetically most stable conformers, all the four titanium atoms are four-coordinated in Ti_4, five equatorial atoms are four-coordinated and two apex atoms are six-coordinated in Ti_7, twelve are six-coordinated and one is twelve-coordinated in Ti_{13}. Although we will invoke the relevance of this coordination number subsequently, it is pertinent to note that the two apex atoms in Ti_7 possess a slightly negative charge as compared to the other five equatorial atoms.[28]

3.1. Dynamics of H_2 Adsorption. The conventional procedure of obtaining the hydrogen adsorption capacities, generally involved the random placement of hydrogen molecules around the metal cluster. Geometry optimizations of several such starting structures resulted in isolating energetically the most stable structures of the metal cluster hydrogen complexes. When the number of hydrogens increases, this procedure is not very effective because hydrogen−hydrogen interactions mar the identification of the energetically or structurally relevant isomers.[48]

In the past, molecular dynamics simulations have been widely used to obtain the sticking probabilities of adsorbates on surfaces.[49] More recently, they have been used to identify the evolution of various cluster structures and also to understand the dissociation mechanism of adsorbates on metal surfaces.[50,51] Although we have carried out a number of trajectories starting from several initial structures, we highlight the relative energies of one such trajectory of the Ti_4H_2 system as a function of the simulation time in the upper panel of Figure 1. The reasons for highlighting this trajectory will be given shortly. At the start of the simulation depicted in Figure 1, the hydrogen molecule was placed at a distance of 5 Å from one of the apex titanium atoms of Ti_4. In the course of the simulation, the hydrogen molecule comes close to the titanium atom and gets dissociated. After dissociation, the hydrogen atoms end up on opposite sides of the Ti−Ti bond. As the simulation time is increased, the hydrogen atoms eventually coalesce and the resulting hydrogen molecule moves away from the Ti_4 cluster. During the entire course of the simulation, the titanium atoms maintain the integrity of the tetrahedral structure of the parent metal cluster albeit with some small changes in the geometries.

It is evident from the energies plotted in Figure 1 that there are several energetic maxima. Two of them, corresponding to simulation times of 20.9 and 28.7 fs merit special mention with respect to the charges of the titanium atom closest to the hydrogen molecule. It can be seen from the lower panel of Figure 1 that the energy maximum around 20.9 fs corresponds to a maximum in the Rydberg charge and the one around 28.7 fs corresponds to a maximum in the valence charge of the titanium atom. This indicates that initially there is a charge transfer from the bonding orbital of the hydrogen molecule to the vacant d orbitals of titanium. After 20.9 fs, the close proximity of the hydrogen molecule to the titanium atom slowly leads to a gradual increase in the valence charge of the titanium atom. However, this process does not go on indefinitely and as

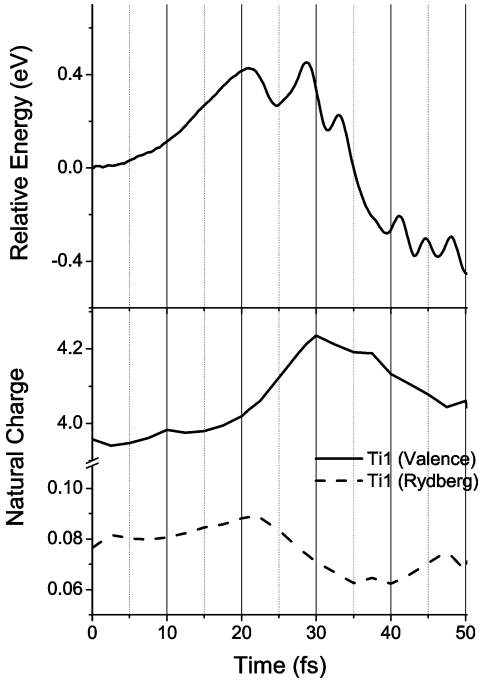

Figure 1. Relative energy (B3LYP/SRECP) of various conformations along the dynamical profile of the Ti_4-H_2 complex. The corresponding valence and Rydberg charges of Ti1 (the titanium atom interacting with the H_2 molecule) are given in the bottom panel.

can be noted from Figure 1, the valence charge gradually decreases after peaking around 30 fs. It can easily be inferred that these two energy maxima correspond to the physisorption (0.42 eV) and chemisorption (0.45 eV) barriers of a single hydrogen molecule on Ti_4. Although these barriers seem to be too low, it is of interest to note that the dissociation−adsorption barrier for a single hydrogen molecule on a Al_{13} cluster was calculated to be ∼0.61 eV (14 kcal/mol).[52]

Although the charges on the titanium atom are affected by its interaction with the hydrogen molecule,[37] it would be more interesting to examine the evolution of the charges on the hydrogen molecule as it approaches the titanium cluster. We employ the AIM method to monitor the charge densities of the entire system at different time steps. Earlier work by one of the authors of this study had shown that compared to conventional analysis of charges, charge density plots are extremely useful in understanding the nature of weak intermolecular interactions and the catalytic role of Lewis acids.[53,54] Before we examine the time evolution of the charge plots, it is useful to compare charge densities obtained using traditional wave function methods and density functional techniques for different electronic states of the bare clusters. This is depicted in Figure 2 for different electronic states of Ti_4 and Ti_7. Figure 2 illustrates that the charge density plots evaluated at both the MP2 and B3LYP levels are very similar. However, this observation requires more investigations using different systems because calculations carried out on isolated CO indicate that electron density distributions obtained using the B3LYP functional are closer to those obtained at the coupled cluster levels of theory than to those at the MP2 level.[55] Figure 2, also indicates that the total charge densities evaluated for different electronic states are also alike. A similar observation has been made in a recent study on electron densities of metastable states.[56] This implies that molecular dynamics simulations involving different electronic states would yield similar results with respect to the charge density plots. However, the calculated dissociation−adsorption

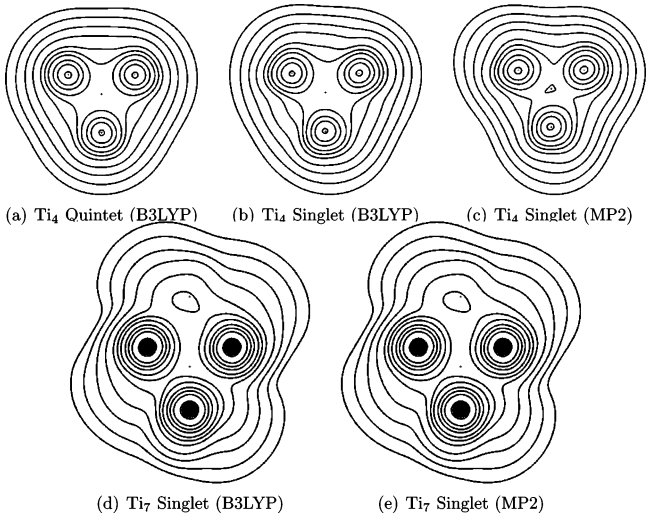

Figure 2. Plots of the electron density (ρ) of different electronic states of Ti_4 and Ti_7 evaluated using the 6-31G* basis set at both the B3LYP and MP2 levels of theory. The contours are drawn in the units of 1, 2, 4, 8×10^n, $n = -3, -2, ..., 1, 2$ au.

energy barriers would not be the same for the different electronic states.

With this background, we examine the charge density plots for the interaction of the hydrogen molecule with the Ti_4 cluster in Figure 3. At the start of the simulation, the hydrogen molecule (5 Å) has only a Coulombic interaction with the titanium cluster. This Coulombic interaction is vital because it dictates on whether a trajectory would eventually lead to a dissociative adsorption of the hydrogen molecule. Consequently, trajectories involving starting structures wherein the hydrogen molecule is collinear to the titanium atom do not lead to either the dissociation or the adsorption of the hydrogen molecule on the titanium cluster. This Coulombic interaction also entails that the hydrogen molecule does not initially interact with the more positively charged equatorial atoms of the Ti_7 cluster. Detailed simulations of the interaction of H_2 with Ti_7 show that H_2 initially approaches and dissociates at the apex titanium atoms and the resulting hydrogen atoms subsequently migrate to equilibrium positions close to the two equatorial titanium atoms. This phenomenon is very similar to "steering effects", which have been ascribed to the high surface reactivity of molecules.[57−59]

Within 10 fs of the dynamics simulation, the hydrogen molecule is about 3.7 Å away from the Ti_4 cluster. Though the charges on both the hydrogen molecule and the metal cluster do not display any perceptible changes, one can notice that there is a significant interaction of the charges. Interestingly, significant van der Waals interaction involving atom−molecule or molecule−molecule systems can also be noted at similar intermolecular separations.[60,61] At 20.9 fs, which corresponds to the onset of the physisorption barrier, the hydrogen molecule is 2.4 Å away from the cluster. Though there is substantial interaction, which is mostly due to a charge transfer from the H−H bond to the vacant titanium d orbitals, the H−H bond length increases by about 0.012 Å. However, the increased charge in the d orbital of one of the titanium atoms and the resulting hybridization lead to a shortening of the Ti−Ti bonds by ∼0.2 Å. At 25 fs, the hydrogen molecule is 2 Å away from the titanium cluster and it undergoes a transition from physisorption to chemisorption. On the basis of the fact that the H−H bond length at this stage is similar to that found at the beginining of the simulation, one can infer that there is a reverse charge transfer from the metal d orbitals to the antibonding orbitals of

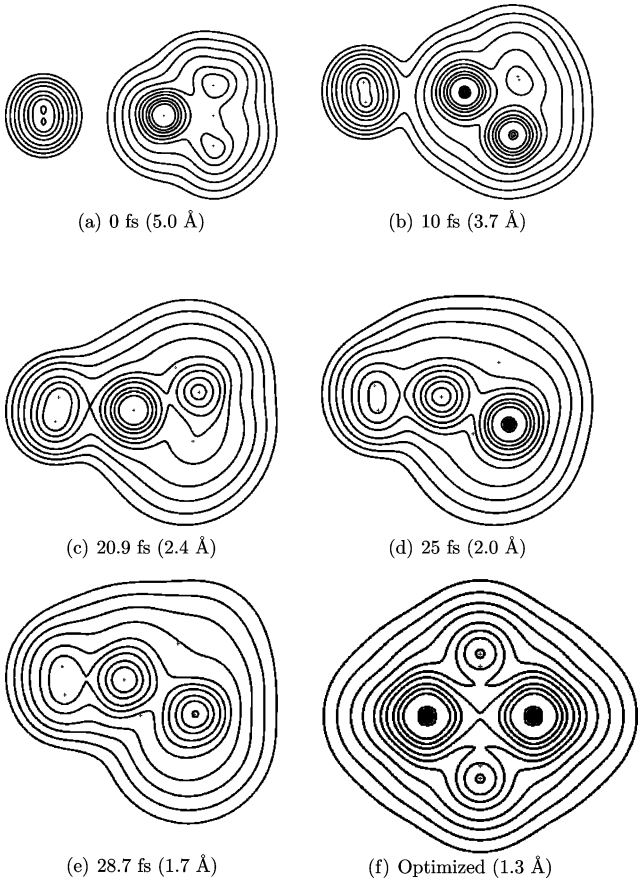

Figure 3. Plots of the electron density (ρ) at different time steps of the molecular dynamics simulation (B3LYP/SRECP) of the Ti_4-H_2 complex. The contours are drawn in the units of 1, 2, 4, 8×10^n, $n = -3, -2, ..., 1, 2$ au.

the hydrogen molecule. The chemisorption barrier occurs at 28.7 fs and the hydrogen molecule is about 1.7 Å away from the titanium cluster. Compared to the initial bond length, the H−H bond increases by about 7.5%. Though no parallels can be drawn, it is interesting to note that in an earlier ab initio study on hydrogen adsorption on an open palladium metal surface, the authors found that the strongest hybridization prevails when the hydrogen molecule is about 1.7 Å away from the palladium atom.[62] There too, the hydrogen molecule was dissociated only when it was directly above a palladium atom on the surface. This seems to indicate that the main driving force for dissociation is due to Pauli repulsion, which is in consonance with earlier observations.[34,35,37] After dissociation, the two hydrogen atoms travel in opposite directions and the equilibrium geometry results from optimization of one of the structures obtained around 50 fs. When the simulation was carried out for long periods of time (~150 fs), the adsorbed hydrogen atoms eventually coalesce, form a hydrogen molecule, and are ejected away from the titanium cluster. This seems to indicate the fluxional nature of hydrogen adsorption on these titanium clusters. This also seems to indicate that in Ti-doped $NaAlH_4$ the aluminum atom would help sequester the hydrogen atoms dissociated by the titanium atom or titanium cluster.

The dynamics simulation carried out on the interaction of the hydrogen molecule with the Ti_7 cluster yielded similar charge profiles. Expectedly, the energy barriers are higher by nearly 1.5 times. However, we do not discuss the detailed dynamics because of a limited number of simulation runs. Additionally, the larger size of the Ti_7 cluster entails that the physisorption and chemisorption barriers appear after longer simulation times. The limited number of dynamics simulations, however, indicate that the dissociation takes place only at the apex titanium atom. This seems to imply that the higher coordination number and the negative charge of the apex titanium atom facilitate hydrogen dissociation. Incidentally, similar observations were made in the correlation of the catalytic activitiy of transition metal surfaces and the coordination number of the constituent metal atoms.[63]

3.2. H_2 Saturation. Because the dynamics simulation enabled the identification of energetically most favored sites for the dissociated hydrogen atoms, we further investigated the structures of the hydrogen saturated small titanium clusters. Our calculations revealed that the hydrogen molecule is always dissociated before it is adsorbed on the titanium cluster. When the titanium cluster is excessively saturated with hydrogen molecules, some of them remain in the molecular form. However, the hydrogen adsorption energies of the resulting clusters are extremely low indicating that adsorption of hydrogen in the molecular form is energetically not favorable.

The bare Ti_4 cluster can exist as either a tetrahedral or a two-dimensional rhombus-like structure. Earlier calculations indicated that the tetrahedral structure is more stable than the rhombus-like structure by about 0.13 eV.[28] Indeed, in the hydrogen saturated Ti_4 clusters (Figure 4), the hydrogen atoms are energetically more stabilized on the tetrahedral clusters (Table 1). It can be seen from Figure 4 and Table 1 that structures in which the hydrogen atom is shared between different titanium atoms are energetically more stable than those in which the hydrogen atom is localized on a single titanium atom. It can be noted from Table 1 that calculations carried out using the larger B3LYP/6-31G** and B3LYP/aug-cc-pVDZ basis sets exhibit energetic trends similar to those for the B3LYP/6-31G* calculations. This is an important observation because it implies that the B3LYP/6-31G* calculational level would yield reliable results in case of the larger hydrogen saturated titanium clusters. Thus, the energetically more stable conformers **462** and **482**, might be responsible for the photoelectron peaks associated with $Ti_4H_6^-$ and $Ti_4H_8^-$.[31]

One of the salient features of these hydrogen saturated titanium structures is the marked tendency for the adsorbed hydrogens to be shared between the different titanium atoms. Irrespective of the cluster size, structures in which the hydrogen atom forms a bond with a single titanium atom are energetically less favored than structures where the hydrogen forms multicenter bonds with the parent titanium cluster. This can be understood from a comparison of the features of structures **481** and **482** illustrated in Figure 4. All the hydrogens in the latter structure are shared between the different titanium atoms and as can be noted from Table 1, **482** exhibits a much larger HOMO−LUMO gap than **481**. Because large HOMO−LUMO gaps are responsible for energetic stability, it can be said that hydrogen multicenter bonds imbue these hydrogen saturated titanium clusters with enhanced energetic stability. It is interesting to note that similar hydrogen multicenter bonds have been recently noted in binary metal oxides.[64,65] Furthermore, the recent work on Al_4H_6 also highlights the role of hydrogen sharing resulting in large HOMO−LUMO gaps and enhanced energetic stability.[66] What is, however, different is that in Al_4H_6, four hydrogens form Al−H bonds and only two hydrogens are shared. On the other hand in the most stable conformer of Ti_4H_6 (**462**), all the hydrogens are shared between the different titanium atoms.

To understand the origin of the enhanced stability of conformer **482** as compared to **481**, it is useful to compare the

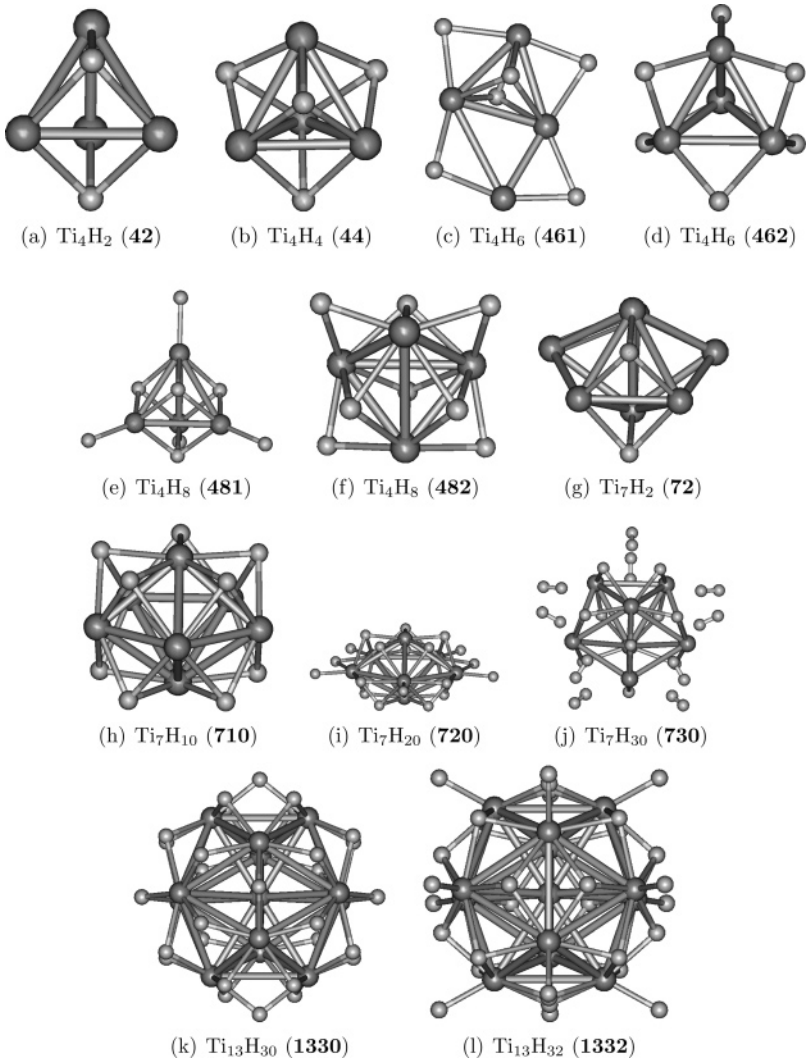

Figure 4. Optimized structures (B3LYP/6-31G*) of some of the Ti_4H_m, Ti_7H_m, and $Ti_{13}H_m$ clusters.

TABLE 1: Calculated (B3LYP) Chemisorption Energies (CE) and HOMO−LUMO (H−L) Gaps of the Ti_4H_m Clusters Investigated in This Study[a]

	6-31G*		6-31G**		aug-cc-pVDZ	
	CE[b]	H−L gap	CE[b]	H−L gap	CE[b]	H−L gap
Ti_4		1.2		1.2		1.2
42	1.92	0.9	1.93	0.9	2.08	0.9
44	2.39	1.5	2.37	1.5	2.31	1.5
461	2.05	1.6	2.01	1.6	1.95	1.4
462	2.68	1.3	2.76	1.3	2.71	1.2
481	1.27	1.1	1.25	1.1	1.23	1.1
482	2.48	1.9	2.44	1.9	2.33	1.8

[a] See Figure 4 for a description of structures. [b] E (eV) = $(2/m)[E(Ti_4) + (m/2)(E(H_2)) - (E(Ti_4{-}H_m))]$.

characteristics of their frontier orbitals with that of the parent Ti_4 and the smaller Ti_4H_4 (**44**) in Figure 5. It can be seen from Figure 5 that the frontier orbitals of both the bare and hydrogenated titanium clusters are entirely composed of metal orbitals (see Supporting Information for the description of all the relevant Ti_4 orbitals). However, the nature of the participating orbitals is quite different. When orbitals are energetically closely placed, it is well-known that symmetry considerations dictate optimal orbital overlap. Thus, for optimal interaction with the multicenter hydrogens, different Ti_4 LUMO's are involved in the interaction in **482**. This in turn influences the energies of the resulting HOMO and LUMO's of **482**. However, the HOMO and LUMO of both **44** and **481** are very similar, indicating that the formation of singly bonded Ti−H molecular species has little influence in changing the Ti−Ti bonding characteristics. The presence of Ti−H bonds, however, lowers the Ti−Ti electron density leading to longer Ti−Ti bonds: 2.746 Å in **481** as compared to 2.519 Å in **44**. It can easily be inferred from the data given in the Supporting Information that the LUMO+2 orbital of the bare Ti_4 cluster becomes the HOMO in **482** and the LUMO+5 orbital of the bare Ti_4 cluster becomes the LUMO in **482**. Of course, this also manifests in the geometries being different with the Ti atoms involved in the HOMO orbital overlap having shorter bond lengths as compared to the other four bonds.

One can extend the characteristics of the frontier orbitals discussed above to the density of states (DOS) and further explain the opening of the gap around the Fermi level in the DOS of the hydrogenated Ti_n clusters.[28] On the basis of the HOMO−LUMO gaps of the bare and hydrogen saturated Ti_n clusters in Tables 1 and 2, it can be noted that the width of the DOS would be substantially increased in the hydrogen saturated clusters. Interestingly, similar observations were made in a recent work on molecular hydrogen adsorption and dissociation on the plutonium surface.[67]

One can note that similar observations can be made in case of the larger Ti_7 and Ti_{13} clusters with the conformers exhibiting hydrogen multicenter bonds being more stable and exhibiting

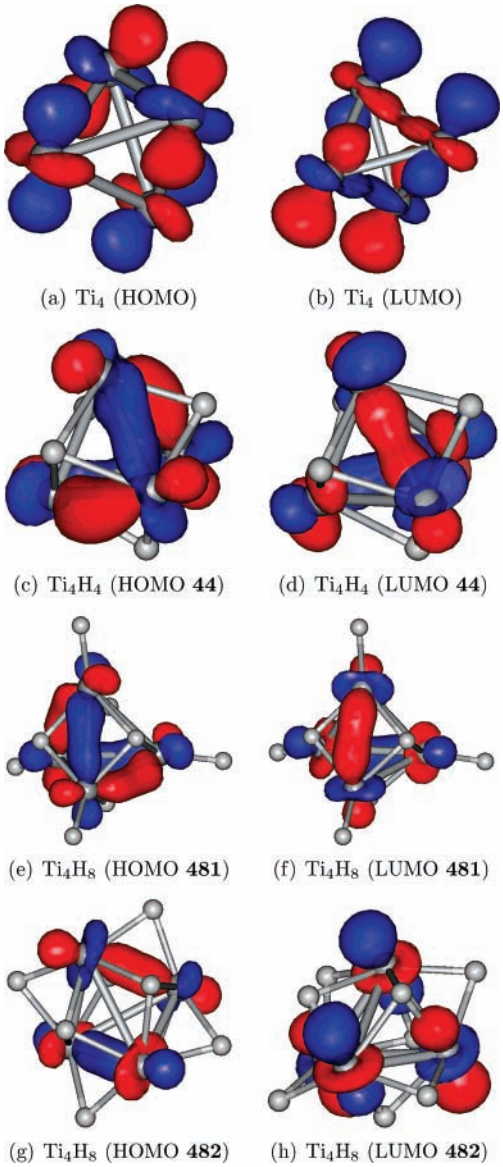

Figure 5. HOMO and LUMO of conformers Ti_4 (singlet), Ti_4H_4 **44**, Ti_4H_8 **481**, and Ti_4H_8 **482**. Note that the LUMO of **482** is entirely localized on the Ti atoms.

TABLE 2: Calculated (B3LYP/6-31G*) Chemisorption Energies (CE) and HOMO−LUMO (H−L) Gaps of the Ti_7H_m and $Ti_{13}H_m$ Clusters Investigated in This Study[a]

	CE[b]	H−L gap
	Ti_7	
Ti_7		1.4
72	2.22	1.3
710	2.00	0.9
720	1.29	1.0
730	0.02	0.3
	Ti_{13}	
Ti_{13}		0.7
1330	1.50	0.9
1332	1.28	1.6

[a] See Figure 4 for a description of structures. [b] E (eV) = $(2/m)[E(Ti_n) + (m/2)(E(H_2)) - (E(Ti_n{-}H_m))]$.

higher chemisorption energies (Figure 4 and Table 2). The case of conformer **1330** is particularly interesting because all the adsorbed hydrogens in it are multicentered. Given the number of adsorbed hydrogens, the resulting chemisorption energy is also very high.

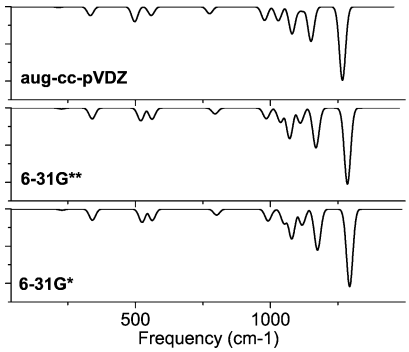

Figure 6. Calculated B3LYP vibrational frequencies of the Ti_4H_8 (**482**) cluster using the 6-31G*, 6-31G**, and aug-cc-pVDZ basis sets.

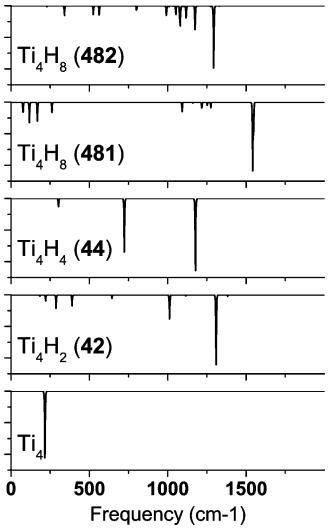

Figure 7. Calculated vibrational frequencies (B3LYP/6-31G*) of the Ti_4, Ti_4H_2 (**42**), Ti_4H_4 (**44**), Ti_4H_8 (**481**), and Ti_4H_8 (**482**) clusters.

The aforementioned discussion leads to the issue of hydrogen saturation limits. The fact that one cannot indiscriminately load hydrogens on these clusters is borne out by calculations on conformer **730**. It can be noted from both the structure (Figure 4) and the corresponding chemisorption energies in Table 2 that most of the hydrogens are not dissociated. This indicates that hydrogen dissociation and hence the corresponding saturation are limited by the optimal coordination number of the titanium atom in the cluster.

3.3. Vibrational Frequencies. To obtain more insight on hydrogen saturation, we computed the vibrational frequencies of the Ti_nH_m clusters. We believe that this would also enable experimentalists to easily monitor the nature of hydrogen saturation. Before we discuss the calculated vibrational frequencies, it is pertinent to mention that all the structures possessing hydrogen multicenter bonds (**482**, **1330**) exhibit no imaginary frequency in the calculated Hessian. On the other hand, the structures possessing singly bonded Ti−H motifs exhibit imaginary frequencies. Though it is not customary to discuss the IR spectra of systems exhibiting imaginary frequencies, we present the spectra of these structure to highlight the significance of hydrogen multicenter bonds.

In Figure 6, we highlight the effect of the basis set on the calculated frequencies of conformer **482** of Ti_4H_8. Except for minor shifts of a few cm^{-1}, the frequencies and intensities obtained using the larger 6-31G** and aug-cc-pVDZ basis sets are nearly similar to those obtained using the 6-31G* basis set.

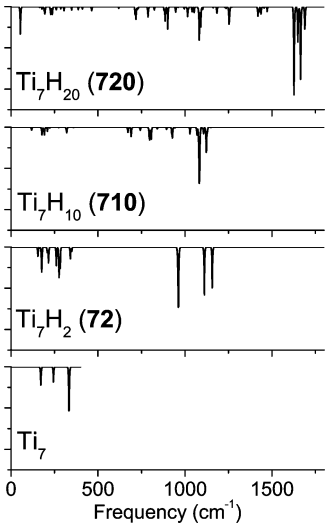

Figure 8. Calculated vibrational frequencies (B3LYP/6-31G*) of the Ti_7, Ti_7H_2 (**72**), Ti_7H_{10} (**710**), and Ti_7H_{20} (**720**) clusters.

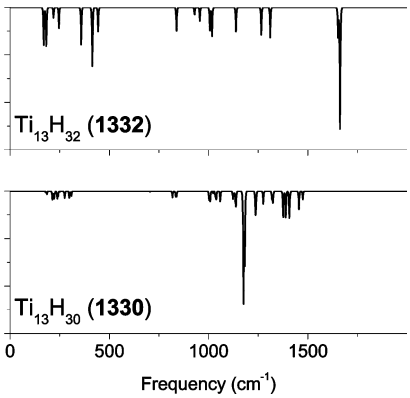

Figure 9. Calculated vibrational frequencies (B3LYP/6-31G*) of the $Ti_{13}H_{30}$ (**1330**) and $Ti_{13}H_{32}$ (**1332**) clusters.

Therefore, in subsequent sections, we only describe the frequencies obtained at the B3LYP/6-31G* level of theory. A recent study indicates that scaling the calculated B3LYP/6-31G* frequencies by a factor of 0.9613 yields good agreement with experiment.[68]

It can be noted from the frequencies plotted in Figures 7 and 8 that all the vibrational modes of both Ti_4 and Ti_7 appear around 350 cm^{-1}. In the absence of any experimental information on the vibrational frequencies of these clusters, it is of interest to note that the Ti−Ti stretching mode appears at 407.9 cm^{-1} in the experimental spectra of the Ti_2 dimer.[69] The bare hydrogen molecule is IR inactive and its physisorption on a metal surface leads to only a weak perturbation in its vibrational spectrum.[70] However, the dissociation of a single hydrogen molecule on Ti_4 leads to strong intense peaks around ∼1000 and ∼1300 cm^{-1} (Figure 7). These modes emerge from the multicenter Ti−H bonds. A comparison of the frequencies of **481** and **482** indicates that the frequencies associated with the singly bonded Ti−H bond appears above 1500 cm^{-1} (Figure 7). This can be seen in more detail in the frequencies of **720** (Figure 8), **1330** and **1332** (Figure 9). A graphical description of the IR intense modes associated with the hydrogen multicenter and singly bonded Ti−H bonds is given in Figure 10. Conformer **1330**, which is entirely composed of hydrogen multicenter bonds exhibits a broad band of IR intense peaks in the 1100−1400 cm^{-1} range. Gomes et al., have reported an IR spectroscopic study of pure, milled, Ti-doped, and hydrogen cycled Ti-doped $NaAlH_4$.[71] It is interesting to note that they observe a broad shoulder in the 1100−1400 cm^{-1} range, which only appears in the hydrogen cycled Ti-doped $NaAlH_4$. The appearance of this broad band was attributed to the AlH_4^- species. However, experimental and theoretical studies of the vibrational spectra of both isolated AlH_4^- and hydrogenated aluminum clusters precludes the appearance of any peak associated with the isolated Al−H mode in the 1000−1500 cm^{-1}.[72−75] It therefore seems more likely that the appearance of this broad shoulder in the hydrogen cycled Ti-doped $NaAlH_4$ can be attributed to the presence of hydrogen multicenter bonds associated with titanium atoms or titanium clusters in the $NaAlH_4$ lattice. Indeed, the presence of titanium clusters in Ti-doped $NaAlH_4$ have been experimentally observed.[22,23,25]

4. Summary and Conclusions

In the course of the current study detailing the nature of hydrogen interaction and saturation on small titanium clusters, we have employed a wide variety of theoretical methods to examine the role of the titanium atom in both dissociating hydrogen molecules and expropriating the dissociated hydrogen atoms.

The ab initio molecular dynamics simulation and the ensuing charge density analysis indicate that the dissociation of the hydrogen molecule primarily results from the Pauli repulsion of the filled *bonding* orbitals of the hydrogen molecule and the titanium s orbital. One of the pertinent findings of this study is that the effect of the titanium atom can be perceived by the hydrogen molecule even at a distance of nearly ∼4 Å. Moreover, the hydrogen molecule is always dissociated before it is adsorbed on the titanium cluster. The hydrogen saturated titanium clusters wherein the hydrogen is in its molecular form are always higher in energy than those in which the hydrogen is dissociated.

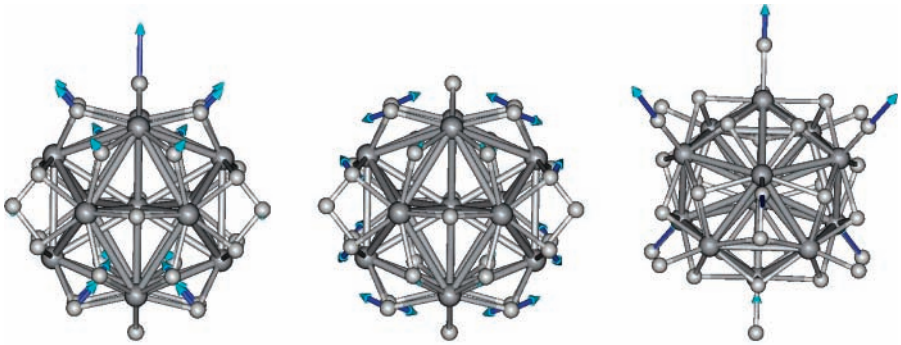

Figure 10. Description of the modes exhibiting the highest IR intensity in the $Ti_{13}H_{30}$ (**1330**) and $Ti_{13}H_{32}$ (**1332**) clusters.

The position of the hydrogen atom in the hydrogen saturated titanium clusters is dictated by the fact that all the titanium atoms of the cluster have a propensity to maximize the charge in their unfilled d orbitals by bonding to an optimal number of hydrogen atoms. The formation of hydrogen multicenter bonds ensures this optimal bonding without breaking any of the Ti−Ti bonds.

Apart from enhancing the stability of the parent titanium cluster, the formation of hydrogen multicenter bonds gives rise to characteristic vibrational modes in the 1100−1400 cm^{-1} range. This is interesting because the vibrational spectra of hydrogen cycled Ti-doped $NaAlH_4$ also yields a broad shoulder in this region. It would therefore be useful to investigate in more detail the vibrational structure of hydrogen saturated metal clusters. Apart from yielding valuable guidelines to experimentalists, such a study would also be useful in readily ascertaining the nature (physisorbed or chemisorbed) of the adsorbed hydrogen.

In light of the observation that the hydrogen storage properties of Ti-doped $NaAlH_4$ is significantly enhanced by using titanium nanoparticles as doping agents,[22] the current study indicates that bare titanium clusters may have a hitherto unexamined role in hydrogen storage.

Acknowledgment. This work was financially supported by Department of Energy (Grant No. DE-FG36-05GO85028).

Supporting Information Available: Orbital descriptions of Ti_4. This material is available free of charge via the Internet at http://pubs.acs.org.

References and Notes

(1) Schlapbach, L.; Züttel, A. *Nature* **2001**, *414*, 353.
(2) Gross, K. J.; Thomas, G. J.; Jensen, C. *J. Alloys Compd.* **2002**, *330−332*, 683.
(3) Jensen, C. M.; Gross, K. J. *Appl. Phys. A* **2001**, *72*, 213.
(4) Schüth, F.; Bogdanović, B.; Felderhoff, M. *Chem. Commun.* **2004**, 2249.
(5) Bérubé, V.; Radtke, G.; Dresselhaus, M.; Chen, G. *Int. J. Energy Res.* **2007**, *31*, 637.
(6) Schüth, F.; Bogdanović, B.; Felderhoff, M. *Chem. Commun.* **2004**, 2249.
(7) Bogdanović, B.; Schiwckardi, M. *J. Alloys Compd.* **1997**, *253−254*, 1.
(8) von Colbe J. M. B.; Felderhoff, M.; Bogdanović, B.; Schüth, F.; Weidenthaler, C. *Chem. Commun.* **2005**, 4732.
(9) Anton, D. L. *J. Alloys Compd.* **2003**, *356−357*, 400.
(10) Chaudhuri, S.; Graetz, J.; Ignatov, A.; Reilly, J. J.; Muckerman, J. T. *J. Am. Chem. Soc.* **2006**, *128*, 11404.
(11) Chaudhuri, S.; Muckerman, J. T. *J. Phys. Chem. B* **2005**, *109*, 6952.
(12) Graetz, J.; Reilly, J. J.; Johnson, J.; Ignatov, A. Y.; Tyson, T. A. *Appl. Phys. Lett.* **2004**, *85*, 500.
(13) Araújo, C. M.; Ahuja, R.; Guillén, J. M. O.; Jena, P. *Appl. Phys. Lett.* **2005**, *86*, 251913.
(14) Araújo, C. M.; Li, S.; Ahuja, R.; Jena, P. *Phys. Rev. B* **2005**, *72*, 165101.
(15) Li, S.; Ahuja, R.; Jena, P. *Phys. Rev. B* **2006**, *73*, 214107.
(16) Marashdeh, A.; Olsen, R. A.; Løvvik, O. M.; Kroes, G.-J. *Chem. Phys. Lett.* **2006**, *426*, 180.
(17) Løvvik, O. M.; Opalka, S. M. *Phys. Rev. B* **2005**, *71*, 054103.
(18) Íñiguez, J.; Yildrim, T. *Appl. Phys. Lett.* **2005**, *86*, 103109.
(19) Wang, P.; Kang, X.-D.; Cheng, H.-M. *J. Phys. Chem. B* **2005**, *109*, 20131.
(20) Liu, J.; Ge, Q. *J. Phys. Chem. B* **2005**, *110*, 25863.
(21) Liu, J.; Ge, Q. *Chem. Commun.* **2006**, 1822.
(22) Bogdanović, B.; Felderhoff, M.; Kaskel, S.; Pommerin, A.; Schlichte, K.; Schüth, F. *Adv. Mater.* **2003**, *15*, 1012.
(23) Fichtner, M.; Fuhr, O.; Kircher, O.; Rothe, J. *Nanotechnology* **2003**, *14*, 778.
(24) Haiduc. A. G.; Stil, H. A.; Schwarz, M. A.; Paulus, P.; Geerlings, J. J. C. *J. Alloys Compd.* **2005**, *393*, 252.
(25) Vegge, T. *Phys. Chem. Chem. Phys.* **2006**, *8*, 4853.
(26) Wang, P.; Jensen, C. M. *J. Alloys Compd.* **2004**, *379*, 99.
(27) Kaldor, A.; Cox, D. M. *J. Chem. Soc., Faraday Trans.* **1990**, *86*, 2459.
(28) Dhilip, Kumar, T. J.; Weck, P. F.; Balakrishnan, N. *J. Phys. Chem. C* **2007**, *111*, 7494.
(29) Feibelman, P. J.; Hamann, D. R. *Solid State Commun.* **1980**, *34*, 215.
(30) Nordlander, P.; Holloway, S.; Nørskov, J. K. *Surf. Sci.* **1984**, *136*, 59.
(31) Burkart, S;, Blessing, N.; Ganteför, G. *Phys. Rev. B* **1999**, *60*, 15639. Kim, Y. D.; Ganteför, G. *J. Mol. Struct.* **2004**, *692*, 139.
(32) (a) Cremaschi, P.; Whitten, J. L. *Phys. Rev. Lett.* **1981**, *46*, 1242. (b) Cremaschi, P.; Whitten, J. L. *Surf. Sci.* **1981**, *112*, 343.
(33) Cremaschi, P.; Whitten, J. L. *Theor. Chem. Acta* **1987**, *72*, 485.
(34) Christmann, K. *Surf. Sci. Rep.* **1989**, *9*, 1.
(35) Harris, J.; Andersson, S. *Phys. Rev. Lett.* **1985**, *55*, 1583.
(36) Hammer, B.; Scheffler, M. *Phys. Rev. Lett.* **1995**, *74*, 3487.
(37) Siodmiak, M.; Govind, N.; Andzelm, J.; Tanpipat, N.; Frenking, G.; Korkin, A. *Phys. Stat. Sol. (B)* **2001**, *226*, 29.
(38) Bauschlicher, C. W., Jr.; Partridge, H.; Langhoff, S. R.; Rosi, M. *J. Chem. Phys.* **1991**, *95*, 1057.
(39) Frisch, M. J.; Trucks, G. W.; Schlegel, H. B.; Scuseria, G. E.; Robb, M. A.; Cheeseman, J. R.; Montgomery, J. A., Jr.; Vreven, T.; Kudin, K. N.; Burant, J. C.; Millam, J. M.; Iyengar, S. S.; Tomasi, J.; Barone, V.; Mennucci, B.; Cossi, M.; Scalmani, G.; Rega, N.; Petersson, G. A.; Nakatsuji, H.; Hada, M.; Ehara, M.; Toyota, K.; Fukuda, R.; Hasegawa, J.; Ishida, M.; Nakajima, T.; Honda, Y.; Kitao, O.; Nakai, H.; Klene, M.; Li, X.; Knox, J. E.; Hratchian, H. P.; Cross, J. B.; Bakken, V.; Adamo, C.; Jaramillo, J.; Gomperts, R.; Stratmann, R. E.; Yazyev, O.; Austin, A. J.; Cammi, R.; Pomelli, C.; Ochterski, J. W.; Ayala, P. Y.; Morokuma, K.; Voth, G. A.; Salvador, P.; Dannenberg, J. J.; Zakrzewski, V. G.; Dapprich, S.; Daniels, A. D.; Strain, M. C.; Farkas, O.; Malick, D. K.; Rabuck, A. D.; Raghavachari, K.; Foresman, J. B.; Ortiz, J. V.; Cui, Q.; Baboul, A. G.; Clifford, S.; Cioslowski, J.; Stefanov, B. B.; Liu, G.; Liashenko, A.; Piskorz, P.; Komaromi, I.; Martin, R. L.; Fox, D. J.; Keith, T.; Al-Laham, M. A.; Peng, C. Y.; Nanayakkara, A.; Challacombe, M.; Gill, P. M. W.; Johnson, B.; Chen, W.; Wong, M. W.; Gonzalez, C.; Pople, J. A. *Gaussian 03*, revision C.02; Gaussian, Inc.: Wallingford, CT, 2004.
(40) Rassolov, V.; Pople, J. A.; Ratner, M.; Windus, T. L. *J. Chem. Phys.* **1998**, *109*, 1223.
(41) Balabanov, N. B.; Peterson, K. A. *J. Chem. Phys.* **2005**, *123*, 064107.
(42) Dolg, M.; Wedig, U.; Stoll, H.; Preuss, H. *J. Chem. Phys.* **1987**, *86*, 866.
(43) Schlegel, H. B.; Millam, J. M.; Iyengar, S. S.; Voth, Daniels, G. A., A. D.; Scuseria, G. E.; Frisch, M. J. *J. Chem. Phys.* **2001**, *114*, 9758. Iyengar, S. S.; Schlegel, H. B.; Millam, J. M.; Voth, G. A.; Scuseria, G. E.; Frisch, M. J. *J. Chem. Phys.* **2001**, *115*, 10291. Schlegel, H. B.; Iyengar, S. S.; Li, X.; Millam, J. M.; Voth, G. A.; Scuseria, G. E. Frisch, M. J. *J. Chem. Phys.* **2002**, *117*, 8694. Schlegel, H. B. *Bull. Korean Chem. Soc.* **2003**, *24*, 1.
(44) Reed, A. E.; Curtiss, L. A.; Weinhold, F. *Chem. Rev.* **1988**, *88*, 889.
(45) Bader, R. F. W. *Atoms in Molecules: A Quantum Theory*; Oxford University Press: New York, 1990. Bader, R. F. W. *Chem. Rev.* **1991**, *91*, 893.
(46) Rao, B. K.; Jena, P.; Burkart, S.; Ganteför, G.; Seifert, G. *Phys. Rev. Lett.* **2001**, *86*, 692.
(47) Huda, M. N.; Ray, A. K. *Phys. Rev. A* **2003**, *67*, 013201.
(48) Chen, B.; Gomez, M. A.; Doll, J. D.; Freeman, D. L. *J. Chem. Phys.* **1998**, *108*, 4031.
(49) Gross, A. In *Computer Simulation of Materials at Atomic Level*; Deák, P., Fraunheim, T., Pederson, M. R., Eds.; Wiley-VCH: Berlin, 2000; Chapter 18, p 389.
(50) Pawluk, T.; Wang, L. *J. Phys. Chem. C* **2007**, *111*, 6713.
(51) Umezawa, N.; Kalia, R. K.; Nakano, A.; Vashista, P.; Shimojo, F. *J. Chem. Phys.* **2007**, *126*, 234702.
(52) Yarovsky, I.; Goldberg, A. *Mol. Simul.* **2005**, *31*, 475.
(53) Tarakeshwar, P.; Kim, K. S. *J. Phys. Chem. A* **1999**, *103*, 9116.
(54) Tarakeshwar, P.; Kim, K. S.; Kraka, E.; Cremer, D. *J. Chem. Phys.* **2001**, *115*, 6018.
(55) He, Y.; Gräfenstein, J.; Kraka, E.; Cremer, D. *Mol. Phys.* **2000**, *98*, 1639.
(56) Legrand, V.; Pillet, S.; Souhassou, M.; Lugan, N.; Lecomte, C. *J. Am. Chem. Soc.* **2006**, *128*, 13921.
(57) Gross, A.; Wilke, S.; Scheffler, M. *Phys. Rev. Lett.* **1995**, *75*, 2718.
(58) Gross, A.; Scheffler, M. *Prog. Surf. Sci.* **1996**, *53*, 187.
(59) Kroes, G.-J.; Gross, A.; Baerends, E.-J.; Scheffler, M.; McCormack, D. A. *Acc. Chem. Res.* **2002**, *35*, 193.
(60) Balakrishnan, N. *J. Chem. Phys.* **2004**, *121*, 5563.
(61) Lee, T.-G.; Balakrishnan, N.; Forrey, R. C.; Stancil, P. C.; Schultz, D. R.; Ferland, G. J. *J. Chem. Phys.* **2006**, *125*, 114302.
(62) Lischka, M.; Gross, A. *Phys. Rev. B* **2002**, *65*, 075420.

(63) Falicov, L. M.; Somorjai, G. A. *Proc. Natl. Acad. Sci. U.S.A.* **1985**, *82*, 2207.
(64) Janotti, A.; van De Walle, C. G. *Nat. Mater.* **2007**, *6*, 44.
(65) Kang, J.; Lee, E.-C.; Chang, K. J.; Jin, Y.-G. *Appl. Phys. Lett.* **2004**, *84*, 3894.
(66) Li, X.; Grubisic, A.; Stokes, S. T.; Cordes, J.; Ganteför, G.; Bowen, K. H.; Kiran, B.; Willis, M.; Jena, P.; Burgert, R.; Schnöckel, H. *Science* **2007**, *315*, 356.
(67) Huda, M. N.; Ray, A. K. *Phys. Rev. B* **2005**, *72*, 085101.
(68) Irikura, K. K.; Johnson, R. D., III; Kacker, R. N. *J. Phys. Chem. A* **2005**, *109*, 8430.
(69) Cossé, C.; Fouassier, M.; Mejean, T.; Tranquille, M.; DiLella, D. P.; Moskovits, M. *J. Chem. Phys.* **1980**, *73*, 6076.
(70) Bellman, J.; Svensson, K.; Andersson, S. *J. Chem. Phys.* **2006**, *125*, 064704.
(71) Gomes, S.; Renaudin, G.; Hagemann, H.; Yvon, K.; Sulic, M. P.; Jensen, C. M. *J. Alloys. Compds.* **2005**, *390*, 305.
(72) Pullumbi, P.; Bouteiller, Y.; Manceron, Y. *J. Chem. Phys.* **1994**, *101*, 3610.
(73) Andrews, L.; Wang, X. *Science* **2003**, *299*, 2049.
(74) Spano, E.; Bernasconi, M. *Phys. Rev. B* **2005**, *71*, 174301.
(75) Goldberg, A.; Yarovsky, I. *Phys. Rev. B* **2007**, *75*, 195403.